This paper is published as part of a PCCP Themed Issue on:
Coarse-grained modeling of soft condensed matter

Guest Editor: Roland Faller (UC Davis)

Editorial

Perspective

Communication

Papers

A coarse-graining procedure for polymer melts applied to 1,4-polybutadiene

T. Strauch, L. Yelash and W. Paul

Received 15th October 2008, Accepted 14th January 2009
First published as an Advance Article on the web 27th January 2009
DOI: 10.1039/b818271j

We present a coarse-graining procedure for homopolymer melts mapping intra- as well as inter-molecular interactions from a chemically realistic united atom description to a bead-spring type molecular model. On the coarse-grained level the repeat units interact through bond-length and bond angle potentials and a non-bonded Lennard-Jones type interaction. The latter one is of the 7,4 form and softer than the typically employed 12,6 interactions. The coarse-graining of the intramolecular interactions follows well developed procedures, however, we point out in which way the non-bonded intramolecular interactions in the chemically realistic model should be treated. The parameters of the non-bonded interaction on the coarse level are determined by matching the zero pressure isobar of the chemically realistic model of a 1,4-polybutadiene melt. For the coarse-grained model we perform melt simulations at several temperatures and compare structural and dynamic properties with the behavior of the chemically realistic model.

1. Introduction

The idea to attempt a mapping between chemically realistic and coarse-grained descriptions of polymers is by now rather old.[1,2] It relies on the universality of polymer behavior, telling us that, for certain properties, chemical detail only determines the prefactors of universal laws[3–5] which one should be able to reproduce simulating not the chemically realistic model but a suitably adapted coarse-grained one. As the coarse-grained model, lattice as well as continuum models have been used[6] and a variety of model polymer systems have been studied (for reviews see ref. 7–10 for the current developments and applications to biopolymers). In other words, coarse-graining can be seen as one step in a renormalization procedure.[11] As with all such procedures, the coarse-graining step defines potentials of mean force, *i.e.*, free energies, on the coarser scale, which normally are many-body potentials[12] not conserving the form of the Hamiltonian. The universality in polymer behavior then tells us that we should be able to approximate the exact potential of mean force through a polymer-type force field involving bonded (bond-length, bond-angle, torsion) and non-bonded (dispersion, Coulomb) forces.

As the coarse-grained potentials are free energies, they depend on the state point at which one wants to perform the simulation. To determine them, one therefore would need to perform a chemically realistic simulation first, which is what one wanted to avoid using the coarse-grained description. For the intramolecular interactions this problem could be solved from the start, again employing a universality in polymer behavior. Melt chains assume random walk configurations on scales larger than the blob size.[3] Isolated chains (*e.g.*, single chains in solution) assume either self-avoiding walk, random walk or collapsed configurations depending on the temperature (solvent quality) at which they are studied. For high temperatures the repulsive part of the interaction dominates and the chains are swollen, for low temperatures the attractive part dominates and the chains are collapsed, and at an intermediate temperature (the Θ-temperature) the two contributions effectively cancel and the chain behaves as a random walk chain on large scales. This is true, when non-bonded interactions between all monomers in the chain are considered, *i.e.*, monomers which are arbitrarily far removed in terms of chemical distance along the chain still experience mutual excluded volume/attraction. When one restricts the non-bonded interaction to a maximum distance along the chain[2] one always obtains Θ configurations and can vary the size of the statistical segment length (corresponding to the blob size in the melt) by the exact choice of the cutoff in chemical distance for the non-bonded interactions. In this way typical melt configurations can be generated by isolated random walk chains from which the intramolecular coarse-grained potentials can therefore be constructed.

Intermolecular interactions were simply chosen purely repulsive in the first coarse-graining attempts[1,13] meaning that these coarse-grained models were not able to reproduce the equation of state of the considered polymer system. One way to improve this was to iteratively optimize the intermolecular interactions in a simulated coarse-grained melt by requiring that the pair distribution function of the chemically realistic melt is reproduced exactly.[14,15] However, this necessarily requires simulations of the underlying chemically realistic model in thermodynamic equilibrium. The obtained parameters are then state point dependent, but one can assume that they are applicable in a certain region around the originally simulated state point. Another approach was followed with the aim to construct coarse-grained models for mixtures of small molecules with oligomers.[16,17] When one assumes that a Lennard-Jones type potential is suitable for the description of non-bonded interactions on the coarse-grained scale, then the position (ρ_c, T_c)

Institut für Physik, Johannes Gutenberg-Universität, Staudinger Weg 7, D-55099 Mainz, Germany

of the liquid-gas critical point of the considered molecule determines the two parameters of the Lennard-Jones model (length scale σ and energy scale ε) uniquely. In this way phase diagrams of mixtures of small molecules including alkane oligomers could be reproduced rather well,[18] even including quadrupolar solvents.[19,20] However, this procedure is not applicable to polymers as their liquid–gas critical point typically lies beyond the limit of their chemical stability. We therefore propose to use equation of state information in the melt for the determination of the non-bonded interaction parameters in this work.

The rest of the manuscript is organized as follows. In section 2 we introduce the chemically realistic model of 1,4-polybutadiene on which the coarse-graining is based and the procedure we followed to determine the bonded and non-bonded interactions on the coarse-grained scale. Section 3 then presents results from Molecular Dynamics simulations of the coarse-grained melt focusing on the question on which scale and how well the structural and dynamical properties of the chemically realistic melt can be reproduced. Finally section 4 gives our conclusions.

2. Coarse-graining procedure

The chemically realistic model for 1,4-polybutadiene that we build our procedure on is a united atom model of a random copolymer of 45% *cis* and 55% *trans* content, so we will not consider vinyl units.[21,22] This model has been tested[23,24] and shown to be able to reproduce experimental data quantitatively without any adjustable parameters (for a review see ref. 25). To define the coarse-grained model, we have to determine bonded as well as non-bonded potentials on the coarse-grained scale. We will be using a mapping where one coarse-grained unit represents one butadiene monomer (see Fig. 1). This mapping of four united atom units into one coarse-grained unit is dictated by chain geometry. The thickness of a polybutadiene chain is roughly 4.5 Å which agrees with the size of the polybutadiene monomer.[27] In this mapping we will not differentiate between *cis* and *trans* units on the coarse-grained scale, so that we have a homopolymer model on that scale. When one performs a separate analysis of, *e.g.*, the distance distribution between adjacent monomers depending on whether one has a *cis–cis*, a *cis–trans* or a *trans–trans* situation, one finds qualitative agreement but some systematic differences. Neglecting these in a mapping to a homopolymer has the advantage that an arbitrary chemical sequence can be reinserted into an equilibrated coarse-grained configuration for remapping to a chemically realistic structure. A similar approach was followed succesfully in ref. 26 in a coarse-graining of atactic polystyrene with about equal probability for both tacticities.

2.1 Bonded interactions

The bonded interactions on the coarse-grained scale can be determined by generating single chains in vacuum using the chemically realistic force-field[23] (with improved torsional parameters in ref. 24). This force field considers all bond lengths to be constrained (l = 1.53 Å for the CH_2–CH_2 bond, l = 1.50 Å for the CH_2–CH bond and l = 1.34 Å for the CH–CH bond). There are two different bond-angle potentials (CH–CH–CH_2 and CH–CH_2–CH_2) and four different torsion potentials (at the double bond differentiating *cis* from *trans*, at the allyl (or α) bond next to the double bond in the *cis* and in the *trans* group, and at the alkyl (or β) bond linking the monomers together. All these degrees of freedom are generated according to their Boltzmann probabilities. *E.g.*, assuming that $U_t(\phi)$ is the rotation potential around the allyl bond in the *trans* group, then

$$P(\phi) = \frac{\int_0^{\phi} \exp\left[\frac{-U_t(\phi')}{k_B T}\right] d\phi'}{\int_0^{2\pi} \exp\left[-\frac{U_t(\phi')}{k_B T}\right] d\phi'} \qquad (1)$$

is the cumulative probability of finding a torsion angle for the allyl bond smaller or equal to ϕ. Drawing a random number $r > 1$ and finding the angle where $P(\phi) = r$ yields this bond angle according to its Boltzmann weight. This procedure is shown in Fig. 2 for the *trans* allyl potential. The curve for the

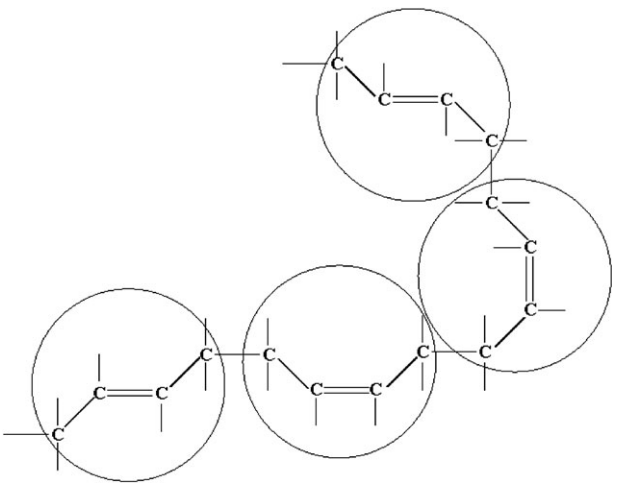

Fig. 1 Sketch of the definition of coarse-grained repeat units for the 1,4-polybutadiene chain.

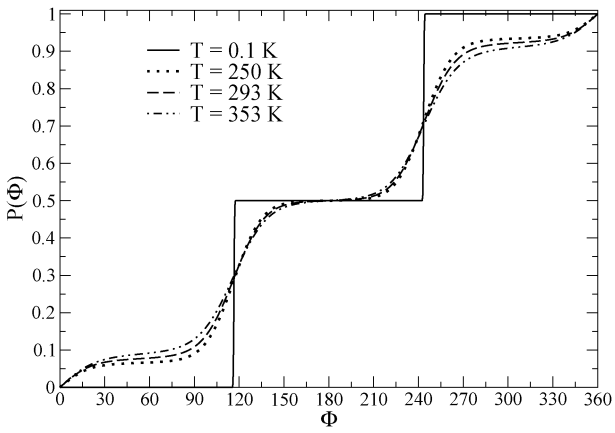

Fig. 2 Cumulative probability distribution for the dihedral angle at the allyl bond in the *trans* monomer for four different temperatures indicated in the legend. The isomeric minima in the corresponding torsion potential around 120° and 240° are isoenergetic.

low temperature (T = 0.1 K), shows that the allyl bond can only assume one of its two isomers (minima in the torsion potential at 120° and 240°) which are isoenergetic. The curves at high temperatures (T = 250 K, T = 293 K and T = 353 K) reveal that there is very little variation of finding a given torsional angle in this temperature range which covers the regime from the high temperature melt to slightly supercooled behavior (the glass transition of this polymer is at T = 180 K). As this holds also true for the other torsional degrees of freedom, and of course also for the bond angles which have force constants of the order of 60 000 K, we can expect little variation of the generated chain structure over this temperature range.

For each such chain we can identify the centers of the monomers and connect them by coarse-grained bonds, thus defining coarse-gained bond lengths, bond angles and dihedral angles, and determine their probabilities. If one does that without consideration of the non-bonded Lennard-Jones interaction between the united atoms in the atomistic chain, one obtains the dotted curves in both parts of Fig. 3. Obviously, the back-folding within this random walk chain gives too much weight to short bond lengths when one compares this curve to the distribution of this length obtained from a coarse-graining of a chemically realistic melt simulation (full curve in the top part), and similarly very small bond angles are allowed (bottom part of Fig. 3). In other words, the single chain generated without taking into account the intramolecular non-bonded interactions has a very different statistical segment length than the melt chains. In order to match this length scale, one has to weight each generated single chain configuration by a Boltzmann factor for non-bonded energy $\exp[-U_{LJ}/k_BT]$, calculated using a suitable cutoff for the non-bonded interactions, not in real space, but according to chemical distance along the chain.[2] The self-consistent way to do this is to include the non-bonded interaction between all pairs of atoms which define a set of bond length, bond angle, and torsion potentials (dashed curves in both parts of Fig. 3). The effect of the other pairwise interactions has to be reproduced through the non-bonded interactions on the coarse-grained scale giving rise to the condensed phase effect on the bond length and bond angle distributions observable as the difference between the dashed and the full curves in Fig. 3. Similar effects would occur for a dihedral angle distribution, of course.

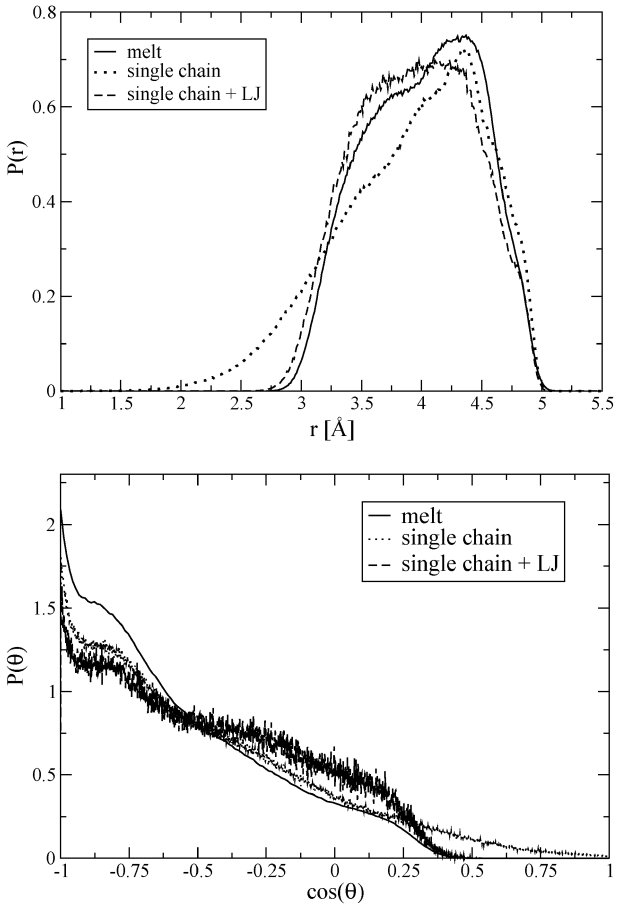

Fig. 3 Top: Probability distribution for the length of bonds between coarse-grained monomers at T = 353 K. The full curve shows the distribution determined from melt configurations of the chemically realistic model. The dotted curve is obtained from single chains where no non-bonded interactions were taken into account as a weight for the Monte Carlo generation of the chain configurations. The dashed curve is obtained when the same configurations are weighted by the non-bonded interactions between all united atoms which make up three consecutive coarse-grained monomers. Bottom: Same as top but for the coarse-grained bond angle distribution.

In our case there is little variation in probability for the coarse-gained dihedral angles, so we choose to work with a coarse-grained model which only included bond length and bond angle potentials. We therefore calculated the Boltzmann weight for each configuration using the Lennard-Jones interactions on the chemically realistic chain between united atoms belonging to three consecutive polybutadiene monomers, which are defining two coarse-grained bond lengths and one coarse-grained bond angle.

The potentials for the coarse-grained bond lengths and bond angles are finally determined from the probability distribution of these coarse-grained degrees of freedom by Boltzmann inversion

$$U(L) = -k_BT \ln[P(L)]$$

$$U(\cos(\Theta)) = -k_BT \ln P(\cos(\Theta)) \quad (2)$$

The resulting potential for the coarse-gained bond length is shown in Fig. 4 and the one for the cosine of the bond angle is shown in Fig. 5. As anticipated, they show little variation over the temperature range studied, with one exception. For the bond length potential a metastable minimum around L = 4.8 Å starts to develop at 250 K. Chain generation at lower temperatures confirms that this minimum deepens at lower temperatures and develops a barrier for transitions between this metastable state and the absolute minimum. One can speculate that this feature leads to a frustration of the bond length at low temperatures indicating a relation with the glass transition of 1,4-polybutadiene. However, to confirm this one would need to perform simulations at lower temperature than we were able to do so far.

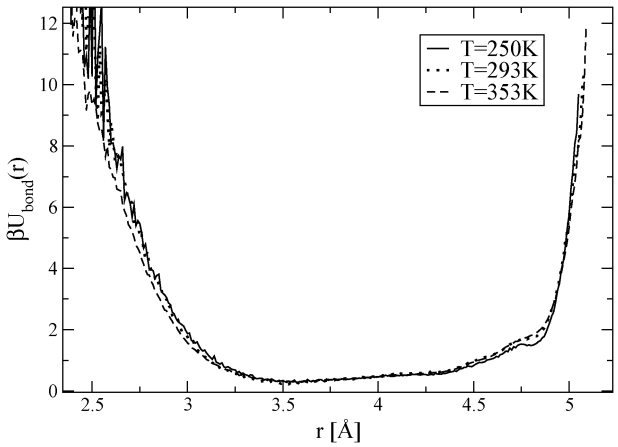

Fig. 4 Effective bond length potential on the coarse-grained level for three temperatures in the melt regime.

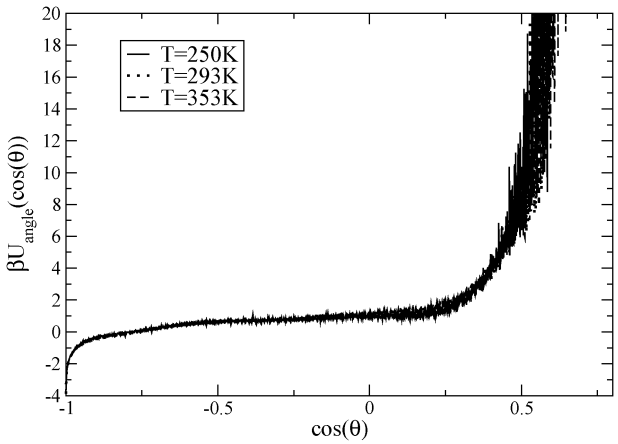

Fig. 5 Effective bond angle potential on the coarse-grained level for three temperatures in the melt regime.

2.2 Non-bonded interactions

For the non-bonded interactions we choose a Lennard-Jones type potential

$$U_{LJ}(r) = 4\varepsilon\left[\left(\frac{\sigma}{r}\right)^n - \left(\frac{\sigma}{r}\right)^m\right]. \qquad (3)$$

From the work in ref. 14 and 15 it is clear that this potential is not able to reproduce intermolecular pair correlations in a polymer melt exactly. The comparison of ref. 27 also showed that the pair correlation in a polybutadiene melt is much less sharply defined than in a bead-spring melt at a corresponding density, when one employs the standard Lennard-Jones potential with $n = 12$ and $m = 6$. The same conclusion was also reached devising a coarse-grained potential for polystyrene.[28] We will therefore work with $n = 7$ and $m = 4$ as in ref. 28.

To determine the Lennard-Jones parameters σ and ε we propose to use equation of state data in the polybutadiene melt, more precisely the zero pressure isotherm. There is probably no one-to-one correspondence between these input data and a set of potential parameters. However, the range of values that σ can assume is restricted, as it has to reproduce the

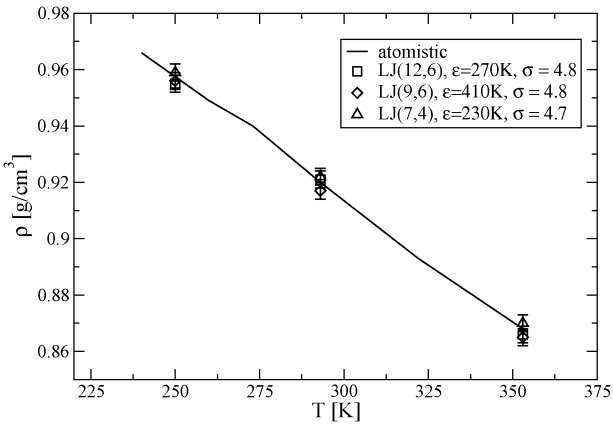

Fig. 6 Zero pressure isobar in the 1,4-polybutadiene melt. The full curve connects results from chemically realistic simulations. The different symbols are average densities in the NpT MC simulation for the optimal choices of parameters for different versions of the Lennard-Jones type interaction (see text).

thickness of the 1,4-polybutadiene chain, *i.e.*, it should be in the approximate range 4.5 Å $\leq \sigma \leq$ 5 Å.

To verify our understanding of the choice of non-bonded potential outlined above, we performed NpT Monte Carlo simulations of the corase-grained melt at $T = 353$ K, $T = 293$ K and $T = 250$ K and zero atmospheres pressure to compare with the zero pressure isobar determined for the chemically realistic model.[29] We did this for three choices of Lennard-Jones type interactions, namely $n = 12, m = 6, n = 9, m = 6$ and $n = 7, m = 4$. Performing simulations for several combinations of σ and ε for all three choices, we can find parameters for which the zero-pressure isobar of the chemically realistic model is reproduced within the errors (see Fig. 6). In all cases, the values obtained for σ and ε are completely reasonable, σ being 4.7 Å or 4.8 Å in the required range, and ε being between 230 K and 410 K. Considering the value of ε for the interaction between two united atoms which is of the order of 100 K, these values are in the right range. As σ is rather constrained in its variation due to the local chain geometry, the main influence on the zero pressure isobars comes from the choice of ε. Changing this parameter one finds that the isobar changes its slope, with the quoted parameters providing the best agreement with the results from the chemically realistic simulations. To distinguish between the different forms for the non-bonded interaction we have to look at the structure of the melt, which we will do for the two extreme cases of (12, 6) and (7, 4) in the next section.

3. Results for the coarse-grained melt

The following results are obtained from NVE Molecular Dynamics simulations of a coarse-gained model employing the potentials determined in section II. We are performing NVE simulations fixing the energy to the average energy at a given temperature obtained from a NVT run using a Langevin thermostat. All simulations were performed for 40 chains of 29 repeat units, which is a coarse-grained representation of the chemically realistic model studied in ref. 21, 22 and 29. The simulations were performed at the densities corresponding to

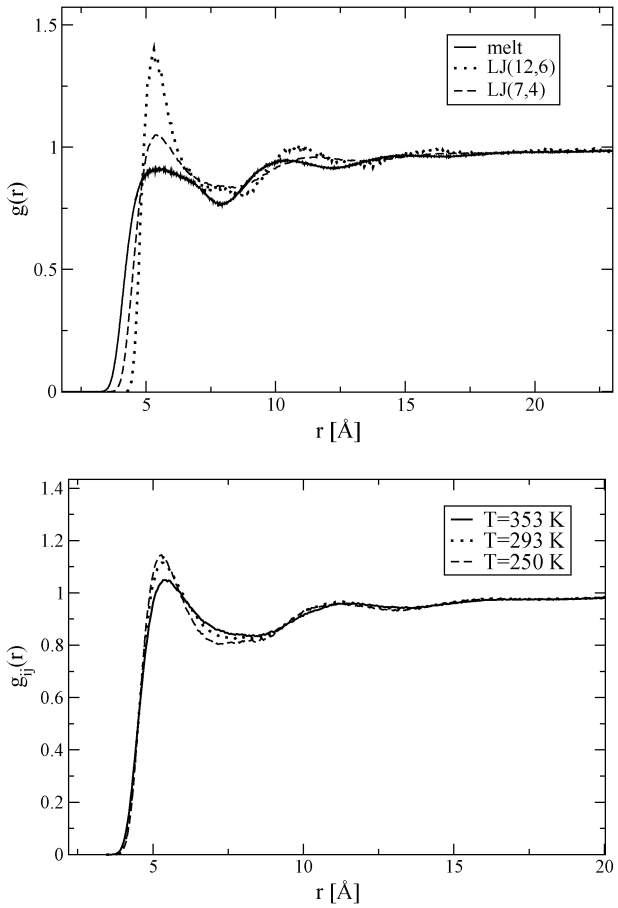

Fig. 7 Top: Intermolecular pair correlation function between centers of coarse-grained monomers in a chemically realistic simulation (full curve) and for simulations of a coarse-grained model using either a 12,6 form of the Lennard-Jones potential (dotted curve) or a much softer 7,4 form (dashed curve). Bottom: Temperature dependence of the intermolecular pair correlation function in a coarse-grained 1,4-polybutadiene melt using the 7,4 Lennard-Jones potential.

the zero-pressure isobar for the chemically realistic model, *i.e.*, we used a box size of linear dimension 48.9 Å at $T = 353$ K, 48.4 Å at $T = 323$ K and 47.2 Å at $T = 240$ K.

For the equilibrated melt we will first look at the structure as revealed by the intermolecular pair-distribution function shown in Fig. 7. The top part of this Figure compares the pair-distribution function between the positions of coarse-grained monomers on different chains as obtained from simulations of the chemically realistic model (full curve)[27] to simulations performed for the coarse-grained model using the 12,6 form of the Lennard-Jones potential (dotted curve) as well as the 7,4 form the potential (dashed curve). The simulations were performed at $T = 353$ K. Clearly, the 12,6 form in the interaction has a much too repulsive core leading to a too-sharp definition of the next-neighbor distance between non-bonded monomers. Due to the coarse-graining, the monomers positioned at the center-of-mass of four united atoms in the chemically realistic chain have a much softer interaction among themselves than the 12,6 form usually employed on the united atom scale. The pair correlation function for the 7,4 form agrees much better with the chemically realistic structure, although, as anticipated, it also gives not an optimal representation of the packing in the 1,4-polybutadiene melt. The bottom part of Fig. 7 shows how the packing between different chains develops as a function of temperature. The first peak sharpens, but the second one changes very little, so that a shallow depletion zone develops at a distance around 8 Å.

Let us now turn to an analysis of the dynamics of the coarse-grained melts. The choice of $\sigma = 4.7$ Å, $\varepsilon = 230$ K and $m = 54$ atomic units for the mass of a butadiene monomer results in a Lennard-Jones time unit

$$\tau_{LJ} = \sqrt{\frac{m\sigma^2}{\varepsilon}} = 2.5\,\text{ps}. \qquad (4)$$

The MD simulation is run with a time increment of $\Delta t = 0.002$ $\tau_{LJ} = 5$ fs, an increase by a factor of 5 compared to typical united atom simulations. With the number of force centers reduced by a factor of 4 and the simpler form of the force-field, we can expect an increase of efficiency of the coarse-grained model compared to the united atom model by a factor of about 30.

Considering our choice of physical properties for fixing the coarse-grained force-field, we would not expect to be able to reproduce the dynamics of the chemically realistic simulations quantitatively. This would entail—in a Rouse model picture—reproducing the segmental friction coefficient in the melt. This is a complex quantity, influenced by intramolecular barriers against rotation as well as by local packing. Especially the former are not captured in our mapping procedure as the chain geometry is only influenced by the minima in the torsion potential and their relative energies. If one would aim to also reproduce the relaxational properties of the underlying chemically realistic model, one would need to include input on local mobilities into the mapping procedure as was done in ref. 1, 30 and 31. In Fig. 8 we show the center-of-mass displacement of chains in the coarse-grained melt. Qualitatively, this behavior reproduces what is known from other coarse-grained or chemically realistic polymer melt

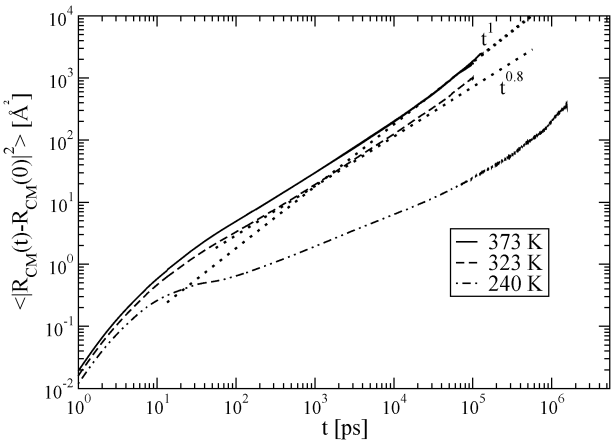

Fig. 8 Mean squared center-of-mass displacement for polymer chains in the coarse-grained model at three different temperatures indicated in the legend. Also shown are power laws indicating a subdiffusive motion for times smaller than the Rouse time and free diffusion at long times. For $T = 240$ K the caging of the monomer-motion sets in, which is observable in the center-of-mass motion of the chains as well.

simulations.[32] There is a subdiffusive regime in the center-of-mass displacement with an exponent around 0.8 which crosses over to Fickian diffusion in the long-time limit. At the lowest temperature a caging regime becomes observable in the center-of-mass mean squared displacement.

An unexpected result is found, when we determine the diffusion coefficient from the long-time limit of the curves in Fig. 8. We obtain $D(373\ \mathrm{K}) \simeq 3 \times 10^{-7}\ \mathrm{cm^2\ s^{-1}}$ $D(323\ \mathrm{K}) \simeq 1.7 \times 10^{-7}\ \mathrm{cm^2\ s^{-1}}$ and $D(240\ \mathrm{K}) \simeq 3 \times 10^{-9}\ \mathrm{cm^2\ s^{-1}}$. The latter value has a large error bar due to the poor statistics of the mean squared displacement for the very long times (more than 1 μs) needed to observe the free diffusion of the chains. These values agree astonishingly well with results for chemically realistic simulations. The value of the diffusion coefficent at $T = 353$ K was determined to be $D(353\ \mathrm{K}) = 3.2 \times 10^{-7}\ \mathrm{cm^2\ s^{-1}}$. At the lower temperatures we only have upper bounds for the diffusion coefficients, $D(323\ \mathrm{K}) \leq 1.8 \times 10^{-7}\ \mathrm{cm^2\ s^{-1}}$ and $D(240\ \mathrm{K}) < 10^{-8}\ \mathrm{cm^2\ s^{-1}}$. The diffusion coefficients at 323 K therefore are in excellent agreement between the chemically realistic and the coarse grained simulations, whereas at higher temperatures the coarse-grained model seems to have a slower dynamics making its center-of-mass diffusion at 373 K equal to the chemically realistic one at 353 K. At the lower temperature the diffusion coefficient for both models is not known with sufficient accuracy for a comparison. Let us therefore look at the translational motion on the level of particle displacements in both models. Of course, in the chemically realistic model, these are united atom displacements and in the coarse-grained model these are displacements of the center-of-mass of a repeat unit of the chemically realistic chain. At short times these two have to disagree, but on time scales where a Rouse model description would be applicable, they both just follow the displacement of a Rouse segment if the segmental friction coefficient in both models agrees. This comparison is performed in Fig. 9. At short times the motion of the united atoms is faster than the one of the monomers. In the ballistic regime for very short times all united atom displacements are quadratic in time.

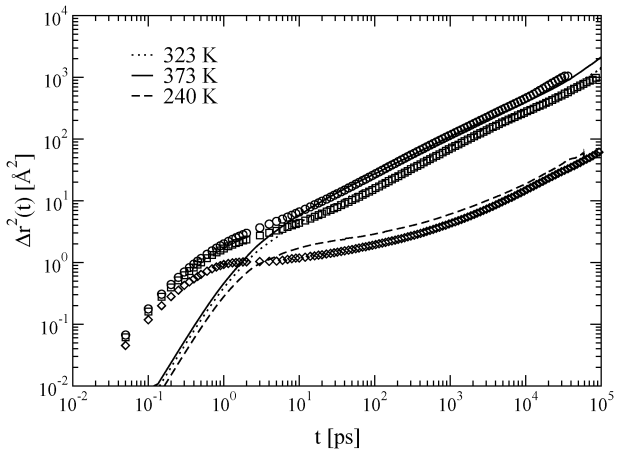

Fig. 9 Average mean-squared monomer-displacement in the coarse-grained polybutadiene melt shown by lines for three different temperatures given in the legend. The symbols are united atom displacements in the chemically realistic simulation at 353 K (top), 323 K (middle) and 240 K (bottom).

However, four united atom displacements have to be added up vectorially to generate a monomer displacement which—assuming the four displacements to be independent—is just one half of the individual displacements. Fig. 9 shows that compared to this simplistic picture, the monomer displacement in the coarse-grained simulation for times of the order of 100 fs is even one order of magnitude smaller than the united atom displacement. For times larger than about 10 ps the monomers displacements and the united atom displacements agree for $T = 323$ K. Furthermore, also the united atom data at 353 K and the coarse-grained data at 373 K agree, as for the diffusion coefficients.

So we can conclude that the segmental friction coefficient at 323 K is reproduced through our mapping—although not being an input to it. For higher temperatures it is larger in the coarse-grained model, whereas it is smaller for lower temperatures. Segmental friction in a polymer melt comes about by packing effects as well as by intramolecular barriers against rotation. As the latter do not influence our mapping procedure we can conclude that the for the temperature regime we are looking at, segemental friction is still largely determined by packing, which we reasonably well reproduce (see Fig. 7). In the simulations of the chemically realistic model it was found that an intramolecular caging due to the torsionial barriers sets in for temperatures below 273 K.[22] Therefore, in the supercooled melt at $T = 240$ K, the cage in the chemically realistic simulation is partly generated by torsional constraints and is smaller (1 Å^2) than in the coarse-grained simulation (about 2 Å^2) where it is also less sharply defined. For this reason, the displacement in the coarse-grained model remains larger than for the chemically realistic model for all times, *i.e.*, the segmental friction in the coarse-grained model, which is not including the effects of intramolecular rotation barriers, is smaller. From this we conclude that the glass transition temperature for the coarse-grained model will be at lower temperatures than for the chemically realistic one. We therefore can expect an increase in speedup for simulations of the coarse-grained model compared to simulations of the chemically realistic model upon lowering the simulation temperature further below 240 K.

4. Conclusions

We have presented a coarse-graining strategy for polymer melts of simple chain architecture and exemplified it for the case of 1,4-polybutadiene. Although this is a copolymer of *cis* and *trans* units, the coarse-grained model we employed is a homopolymer one. The force-field consists of bonded and non-bonded interactions. For the determination of the bonded interactions we employed the Flory conjecture that melt chains obey random walk statistics (it has recently been shown that this is not strictly true[33]). We can therefore generate single random walk chains using the chemically realistic model, weighted by the appropriate non-bonded (*i.e.* Lennard-Jones) interactions in the chemically realistic force field. We pointed out that for self-consistency reasons one has to take all non-bonded interactions within groups of atoms defining bonded coarse-grained interactions into account when calculating this weight. The determination of the bonded coarse-grained force

field therefore does not need any melt simulations of the chemically realistic model.

This is no longer true for the determination of the non-bonded part of the coarse-grained force field. There are several strategies in the literature how to determine the non-bonded forces. We suggest here a new approach where we choose a soft Lennard-Jones type form of the non-bonded interaction potential and match isobars between chemically realistic and coarse-grained simulations. It was found in general, that the softer Lennard-Jones type potential yields a better representation of the melt packing than the typically employed (12,6) Lennard-Jones potential.

With the force field fixed in this way, we obtain a good agreement in the size of the melt chains and the melt structure between chemically realistic and coarse-grained simulations. The longest relaxation time in the two models agrees at $T = 323$ K, whereas the coarse-grained model shows slower relaxation at higher temperatures and faster relaxation at lower temperatures. We conclude that the relaxation in the high temperature regime is dominated by packing which is reproduced in the mapping leading to this agreement in relaxation times. At lower temperatures (below 273 K), however, intramolecular barriers against rotation strongly influence the dynamics in the chemically realistic model. As these are absent in the coarse-grained model the segmental friction coefficient in the coarse-grained model becomes smaller than in the chemically realistic model. This will go along with a reduction in glass transition temperature of the coarse-grained model compared to the chemically realistic one, leading to an increasing gain in efficiency when employing the coarse-grained model with decreasing temperature. Where exactly the glass transition temperature of this model lies has to be studied with further simulations at lower temperatures. It would also be interesting to find extensions of the mapping able to match the glass transition temperature between the two descriptions of the same polymer.

References

1 W. Paul, K. Binder, K. Kremer and D. W. Heermann, *Macromolecules*, 1991, **24**, 6332.
2 J. Baschnagel, K. Binder, W. Paul, M. Laso, U. W. Suter, I. Batoulis, W. Jilge and T. Bürger, *J. Chem. Phys.*, 1991, **95**, 6014.
3 P. G. de Gennes, *Scaling Concepts in Polymer Physics*, Cornell University Press, Ithaca, 1996.
4 M. Doi and S. F. Edwards, *The Theory of Polymer Dynamics*, Oxford University Press, Oxford, 1986.
5 A. Y. Grosberg and A. R. Khokhlov, *Statistical Physics of Macromolecules*, AIP Press, New York, 1994.
6 J. Baschnagel, K. Binder, P. Doruker, A. A. Gusev, O. Hahn, K. Kremer, W. L. Mattice, F. Müller-Plathe, M. Murat, W. Paul, S. Santos, U. W. Suter and V. Tries, *Adv. Polym. Sci.*, 2000, **152**, 41.
7 *Simulation Methods for Polymers*, ed. M. Kotelyanski and D. N. Theodoru, Marcel Dekker, New York, 2004.
8 F. Müller-Plathe, *ChemPhysChem*, 2002, **3**, 754.
9 M. Praprotnik, L. Delle Site and K. Kremer, *Ann. Rev. Phys. Chem.*, 2008, **59**, 545.
10 *Coarse-Graining of Condensed and Biomolecular Systems*, ed. G. Voth, Taylor and Francis, Abdingdon, 2008.
11 W. Paul, in *Proceedings of the NATO Advanced Research Workshop on Multiscale Computational Methods in Chemistry and Biology*, ed. A. Brandt, J. Bernholc and K. Binder, IOS Press, Amsterdam, 2001.
12 W. G. Noid, J.-W. Chu, G. S. Ayton, V. Krishna, S. Izekov, G. A. Voth, A. Das and H. C. Andersen, *J. Chem. Phys.*, 2008, **128**, 244114; W. G. Noid, P. Liu, Y. Wang, J.-W. Chu, G. S. Ayton, S. Izekov, H. C. Anderson and G. A. Voth, *J. Chem. Phys.*, 2008, **128**, 244115.
13 W. Tshoep, K. Kremer, J. Batoulis, T. Bürger and O. Hahn, *Acta Polym.*, 1998, **49**, 68; W. Tschoep, K. Kremer, O. Hahn, J. Batoulis and T. Bürger, *Acta Polym.*, 1998, **49**, 75.
14 H. Meyer, O. Biermann, R. Faller, D. Reith and F. Müller-Plathe, *J. Chem. Phys.*, 2000, **113**, 6264.
15 D. Reith, M. Pütz and F. Müller-Plathe, *J. Comput. Chem.*, 2003, **24**, 1624.
16 K. Binder, M. Müller, P. Virnau and L. G. MacDowell, *Adv. Polymer Sci.*, 2005, **173**, 1.
17 B. M. Mognetti, P. Virnau, L. Yelash, W. Paul, K. Binder, M. Müller and L. G. MacDowell, *J. Chem. Phys.*, 2009, **130**, in press.
18 Kurt Binder, Wolfgang Paul, Peter Virnau, Leonid Yelash, Marcus Müller and Luis Gonzalez MacDowell, in *Coarse-Graining of Condensed and Biomolecular Systems*, ed. G. Voth, Taylor and Francis, Abingdon, 2008.
19 B. M. Mognetti, M. Oettel, L. Yelash, P. Virnau, W. Paul and K. Binder, *Phys. Rev. E*, 2008, **77**, 041506.
20 B. M. Mognetti, L. Yelash, P. Virnau, W. Paul, K. Binder, M. Müller and L. G. MacDowell, *J. Chem. Phys.*, 2008, **128**, 104501.
21 S. Krushev, W. Paul and G. D. Smith, *Macromolecules*, 2002, **35**, 4198.
22 S. Krushev and W. Paul, *Phys. Rev. E*, 2003, **67**, 021806.
23 G. D. Smith and W. Paul, *J. Phys. Chem. A*, 1998, **102**, 1200.
24 G. D. Smith, W. Paul, M. Monkenbush, L. Willner, D. Richter, X. H. Qiu and M. D. Ediger, *Macromolecules*, 1999, **32**, 8857.
25 W. Paul and G. D. Smith, *Rep. Prog. Phys.*, 2004, **67**, 1117.
26 Q. Sun and R. Faller, *Macromolecules*, 2006, **39**, 812.
27 L. Yelash, M. Müller, W. Paul and K. Binder, *J. Chem. Theory Comput.*, 2006, **2**, 588.
28 V. A. Harmandaris, D. Reith, N. F. A. Van der Vegt and K. Kremer, *Macromol. Chem. Phys.*, 2007, **208**, 2109.
29 S. Krushev, *Computersimulationen zur Dynamik und Statik von Polybutadienschmelzen*, Universität Mainz, PhD Thesis (unpublished), 2002.
30 W. Paul and N. Pistoor, *Macromolecules*, 1994, **27**, 1249.
31 V. Tries, W. Paul, J. Baschnagel and K. Binder, *J. Chem. Phys.*, 1997, **106**, 738.
32 W. Paul, *Chem. Phys.*, 2002, **284**, 59.
33 J. P. Wittmer, H. Meyer, J. Baschnagel, A. Johner, S. P. Obukhov, L. Mattioni, M. Müller and A. N. Semenov, *Phys. Rev. Lett.*, 2004, **93**, 147801; J. P. Wittmer, P. Beckrich, A. Johner, A. N. Semenov, S. P. Obukhov, H. Meyer and J. Baschnagel, *Europhys. Lett.*, 2007, **77**, 56003; J. P. Wittmer, P. Beckrich, A. Cavallo, A. Johner and J. Baschnagel, *Phys. Rev. E*, 2007, **76**, 011803.

